

## UNDERSTANDING SPACE WEATHER

Author(s): Keith T. Strong, Joan T. Schmelz, Julia L. R. Saba and Therese A. Kucera

Source: *Bulletin of the American Meteorological Society*, Vol. 98, No. 11 (NOVEMBER 2017), pp. 2387-2396

Published by: American Meteorological Society

Stable URL: <https://www.jstor.org/stable/10.2307/26396328>

## REFERENCES

Linked references are available on JSTOR for this article:

[https://www.jstor.org/stable/10.2307/26396328?seq=1&cid=pdf-reference#references\\_tab\\_contents](https://www.jstor.org/stable/10.2307/26396328?seq=1&cid=pdf-reference#references_tab_contents)

You may need to log in to JSTOR to access the linked references.

---

JSTOR is a not-for-profit service that helps scholars, researchers, and students discover, use, and build upon a wide range of content in a trusted digital archive. We use information technology and tools to increase productivity and facilitate new forms of scholarship. For more information about JSTOR, please contact support@jstor.org.

Your use of the JSTOR archive indicates your acceptance of the Terms & Conditions of Use, available at <https://about.jstor.org/terms>



American Meteorological Society is collaborating with JSTOR to digitize, preserve and extend access to *Bulletin of the American Meteorological Society*

JSTOR

# UNDERSTANDING SPACE WEATHER

## Part II: The Violent Sun

KEITH T. STRONG, JOAN T. SCHMELZ, JULIA L. R. SABA, AND THERESE A. KUCERA

Understanding the causes of short-term solar variability may help in developing capabilities to predict and mitigate the impacts of space weather on our increasingly technological society.

Solar radiation can vary across the entire electromagnetic spectrum on time scales from seconds (flares) to decades (the solar cycle). An example of an eruptive flare, which is an event that is a combination of a flare and a coronal mass ejection (CME), is shown in Fig. 1.

This paper is the second in a series of five papers about understanding the phenomena that cause space weather and their impacts. These papers are a primer for meteorological and climatological students who may be interested in the outside forces that can directly or indirectly affect Earth's neutral atmosphere. The

series is also designed to provide background information for the many media weather forecasters who often refer to solar-related phenomena such as flares, CMEs, coronal holes, and geomagnetic storms. Often those presentations are misleading or definitively wrong. Our intention is to provide a basic context so that students and media meteorologists can produce more informative and interesting program content with respect to space weather.

Strong et al. (2012, hereafter Part I) described the production of solar energy and its tortuous journey from the solar core to the surface. That paper dealt with long-term variations of the solar output. This paper (Part II) deals with short-term solar variability (primarily flares and CMEs). Strong et al. (2017, hereafter Part III) will discuss the outflow of particles from the Sun in the form of the solar wind and how it flows throughout the entire solar system. The forthcoming Part IV ("The Sun-Earth Connection") will deal specifically with how variable solar output interacts with the outer layers of Earth's atmosphere. Part V ("Impacts on Life and Society") will discuss the tangible effects of space weather on our increasingly technology-dependent civilization.

**THE SOLAR ATMOSPHERE.** Just as Earth's atmosphere contains layers such as the troposphere and stratosphere, the solar atmosphere is made up of four distinct layers: the photosphere, chromosphere,

**AFFILIATIONS:** STRONG\* AND SABA\*—University of Maryland, College Park, College Park, and NASA Goddard Space Flight Center, Greenbelt, Maryland; SCHMELZ—Universities Space Research Association, Columbia, Maryland, and University of Memphis, Memphis, Tennessee; KUCERA—NASA Goddard Space Flight Center, Greenbelt, Maryland

\* Emeritus

**CORRESPONDING AUTHOR:** Dr. Keith T. Strong, drkts@aol.com

*The abstract for this article can be found in this issue, following the table of contents.*

DOI:10.1175/BAMS-D-16-0191.1

In final form 13 April 2017

©2017 American Meteorological Society

For information regarding reuse of this content and general copyright information, consult the [AMS Copyright Policy](#).

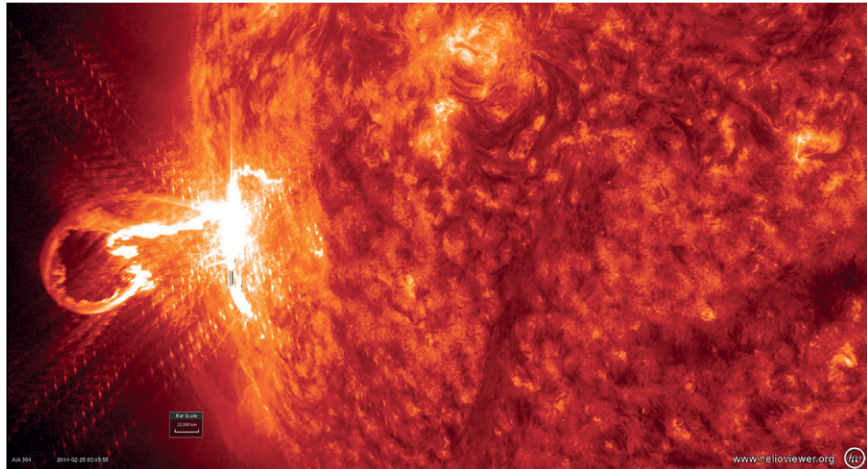


**FIG. 1.** An X5 flare at 0046 UTC 25 Feb 2014 on the eastern limb of the Sun taken in He II (30.4 nm). This is the third largest flare of solar cycle 24. The flare is accompanied by a major eruption of dense, cool plasma and a CME (Fig. 6). The diagonal patterns are caused by diffraction off the instrument's thermal filter support grid. [Source: National Aeronautics and Space Administration (NASA) SDO Atmospheric Imaging Assembly (AIA).]

transition region, and corona. Each is characterized by its temperature structure, density distribution, composition, and magnetic properties. However, it is a mistake to consider the layers as isolated since they are intimately linked via the energy transport and dynamics of the various physical phenomena that propagate through them.

The density of the solar plasma in the interior decreases with increasing distance from the core, reducing the opacity of the plasma and thus increasing the mean free path of photons. When the optical depth of the plasma falls to  $<0.7$  for optical wavelengths, those photons are free to escape into interplanetary space. The layer where that happens, the visible surface of the Sun as we see it in the sky, is called the photosphere. It appears solid and sharply defined from afar but is no more so than the top of a cloud.

The photosphere has a temperature of about 5,800 K and a density of about  $2 \times 10^{-4} \text{ kg m}^{-3}$ , or about 0.02% of the density of Earth's atmosphere at sea level. At these temperatures, the peak of the solar emission spectrum is about 500 nm, which makes the Sun a star of spectral type G2V. Although the Sun is emitting more green photons than any other visible wavelength, it appears white in space. As a result of disproportionate atmospheric attenuation of the blue end of the solar spectrum, the Sun can appear to have any color from yellow to red depending on how high it is in the sky and on atmospheric conditions.

The composition of the photosphere is similar to that of the deeper layers of the Sun because of the continual churning of the convection zone (see Part I) that keeps

the plasma well mixed. Its primary components (by mass) are hydrogen (71%) and helium (27%), with trace amounts of oxygen, carbon, neon, iron, and other heavier elements (Asplund et al. 2009). The elemental abundances in the photosphere are determined from radiative transfer models of the dark absorption lines seen in the solar spectrum (i.e., the Fraunhofer lines).

The most obvious features in the photosphere are sunspots. These are areas where strong magnetic fields (up to 4,000 G, about 10,000 times that of Earth's surface magnetic field) generated in

the solar interior protrude through the photosphere up into the corona. Sunspots appear dark because the presence of strong magnetic fields inhibits the outward flow of energy to the surface by convection. Thus, sunspots receive less energy and so are about 2,000 K cooler than the surrounding photosphere and appear dark by contrast. Sunspots come in all sizes and shapes from tiny individual pores to huge spots with vast penumbras many times the size of Earth. The penumbra of a sunspot is the lighter area surrounding the dark umbra (see, e.g., Fig. 6 in Part I). However, the magnetic fields in the photosphere are not confined to sunspots. There is an intricate network of weaker fields, often referred to as the quiet sun, of 100 G or more (Fig. 2).

The density of the photospheric plasma is sufficiently high that the plasma pressure exceeds the magnetic pressure in the sunspots and so controls the motions of any magnetic fields embedded in the photosphere; the churning motions of the photosphere serve to weave and stress the magnetic fields and thus, by storing energy in the fields, create the opportunity for them to become unstable and erupt violently in the form of a flare or a CME. Flares are predominantly thermal emissions from comparatively dense, hot ( $>1 \text{ MK}$ ) plasma trapped in strong magnetic fields whereas a CME is mostly the expulsion of a large mass of cool ( $\sim 50,000 \text{ K}$ ) plasma from the Sun. The stronger fields in sunspot regions can give rise to large flares and CMEs, but CMEs can also originate from the eruption of filaments in regions of quiet Sun.

As the temperature and density continue to decrease above the photosphere, the solar plasma reaches

its temperature minimum (4,500 K). This lies in the middle of the layer called the chromosphere, an approximately 2,000-km-thick layer (see Fig. 2 in Part I). At the top of this layer, the solar atmosphere has a density of only  $10^{-11}$  kg m $^{-3}$ . This compares to the density of Earth's atmosphere of about 1.5 kg m $^{-3}$  at sea level and  $1.3 \times 10^{-5}$  kg m $^{-3}$  at an altitude of 80 km. The chromospheric temperature, however, changes in a completely unexpected way: above the temperature minimum, it begins to rise to as high as 25,000 K at the top of the chromospheric layer.

The discovery of the increasing temperature gradient of the upper chromosphere originally shocked the scientific world as it seemed to contradict the laws of thermodynamics. The first spectrum of the chromosphere was obtained during the total solar eclipse of October 1888. A prominent yellow line visible in the spectrum could not be attributed to any material known at the time. Norman Lockyer suggested that the yellow line was emitted by a new element—helium—which turned out to be the second most common element in the universe (after hydrogen).

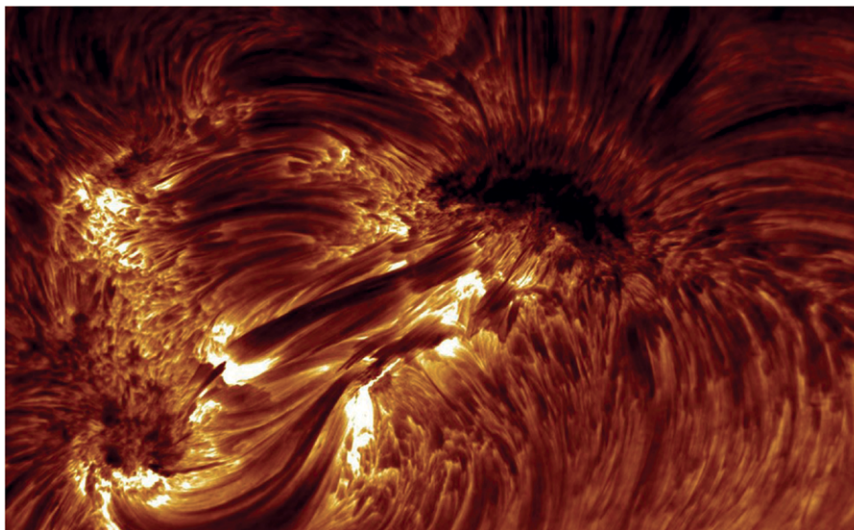


**FIG. 3.** The magnetic complexity in the solar chromosphere near a large sunspot is revealed by plasma-filled loops as seen in H $\alpha$  (656.28 nm) from the Swedish 1-m Solar Telescope on La Palma in the Canary Islands.

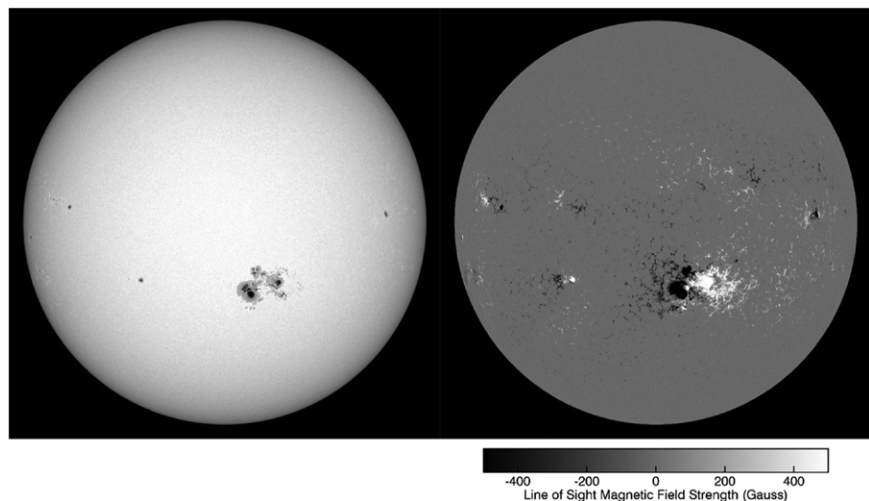


**FIG. 2. (left)** A white-light image of the Sun on 23 Oct 2014 showing the largest sunspot observed in over two decades and (right) a simultaneous magnetogram of the same regions. About 50 Earths would fit into this sunspot group. However, there are large areas of weaker magnetic fields spread across the Sun well away from the sunspots. Note how each sunspot has an area of both positive (white) and negative (black) magnetic field associated with it. [Source: NASA SDO Helioseismic and Magnetic Imager (HMI).]

The low-temperature chromosphere is visible through narrowband optical filters tuned to the red line of the hydrogen spectrum: the H $\alpha$  line. This window into the solar atmosphere clearly shows the complex magnetic structures that suffuse the chromosphere (Fig. 3). The higher-temperature region of the chromosphere also radiates at much shorter wavelengths. Therefore, detectors sensitive to UV and extreme ultraviolet (EUV) photons are needed to image the upper layers of the chromosphere, and as those photons are absorbed by our atmosphere, the detectors must be placed in space.

The chromosphere reveals a variety of dynamic features associated with the complex magnetic fields that permeate the region. Long, narrow jets called spicules (see Fig. 4) hurl dense, cool photospheric plasma at speeds of up to 30 km s $^{-1}$  high into the solar atmosphere above the chromosphere (De Pontieu et al. 2007). It is estimated that there are hundreds of thousands of these covering about 1% of the solar

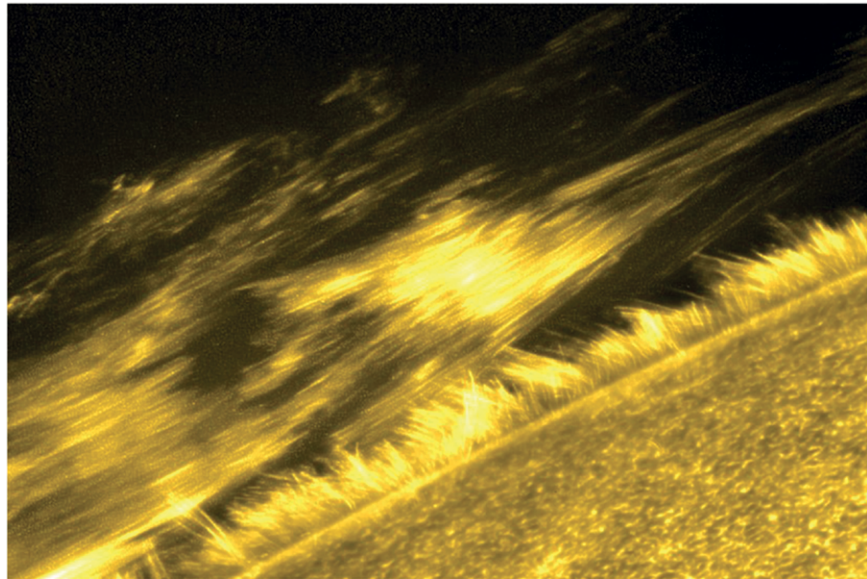


**FIG. 4. An image of the solar limb showing spicules and part of an overlying prominence. Spicules are less than 1,000 km wide and can reach to heights of about 10,000 km above the photosphere. [Source: Japan Aerospace Exploration Agency (JAXA)/NASA/Hinode/Solar Optical Telescope (SOT).]**

surface, and their upward mass transport is many times that of the solar wind.

Chromospheric material can stretch high into the solar atmosphere in the form of filaments and prominences (Mackay et al. 2010). These are vertical sheet-like structures that can stretch as far as 800,000 km across the Sun's surface and as much as 100,000 km high. When seen on the disk, they appear like dark ribbon structures lying along magnetic neutral lines (i.e., the demarcation lines between regions of opposite polarity) and are referred to as filaments. They appear dark because they are sufficiently cool and dense that they absorb the light emitted from the underlying plasma. When on the limb these same structures appear bright against the dark-sky background and are called prominences (Fig. 5).

Filaments can last from a few hours to many months. How these dense, cool structures can remain stable when surrounded by hot coronal plasma perplexed solar physicists for a long time. It is now believed that they are supported by concave (sagging) magnetic arcades of loops and are insulated from the high-temperature corona by the magnetic fields that encase them. When the magnetic fields supporting and overlying these structures become unstable, the filaments and prominences can erupt violently, producing a CME (Fig. 6). Observations show that filaments seem to be extremely dynamic with continuous strong downflows. This then poses the question: where does their mass come from and how is it resupplied?

The mass is much greater than that available from the surrounding corona. One possibility is that the mass is supplied by spicules, but this has not yet been established.

Above the chromosphere is the transition region, a layer about 100 km thick. The temperature increases sharply as the density plummets, which changes the magnetic properties of the outer layers of the solar atmosphere. The magnetic pressure now dominates the plasma pressure, so the magnetic field channels the motion of the plasma higher in the solar atmosphere. This explains why magnetic loop structures are clearly visible in

images of the high-temperature corona. All elements are ionized in this region, and the charged particles can only follow the field lines, not cross them save by a slow diffusion process. Even the solar elemental abundances can change under these conditions (Schmelz 1999).

Above the transition region lies the corona, which from the ground can be best observed during a total solar eclipse. This is possible because the intense light emitted by the photosphere scatters off both electrons and dust particles. During the total solar eclipse of 7 August 1869, a new green line was observed in the visible-light spectrum. Like helium, this line was thought to be from an as-yet unknown element, provisionally named coronium. As the periodic table began to fill up, however, there was no place left to put this new element.

Walter Gotrian and Bengt Edlén later discovered that this green line resulted from highly ionized iron (Fe XIV: an iron atom with 13 electrons missing), not from a new element. But with this identification came another startling discovery: the only reasonable way for the solar corona to create this ion was for it to have temperatures in excess of 1 MK! These soaring temperatures indicate that the corona is a source of light with even higher energies than the UV, so the corona glows brightly in EUV and X-rays.

The corona appears highly structured as the glowing high-temperature plasma traces out the closed magnetic fields in a dazzling and bewildering forest

of coronal loops connecting opposite magnetic polarities on the solar surface (see Fig. 1 in Part I). Some magnetic areas connect directly to the interplanetary fields; these are open field lines that allow the plasma to escape out into the solar system in the form of the solar wind. As these open coronal structures have both lower temperatures and densities, they emit fewer X-rays and appear much darker than the rest of the corona and are referred to as coronal holes (Fig. 7).

How can the corona be so hot? Most solar physicists agree that the reasons are related to the stressed magnetic field. Since the corona has such low densities (lower than the best vacuums achievable on Earth), only a small fraction of available magnetic

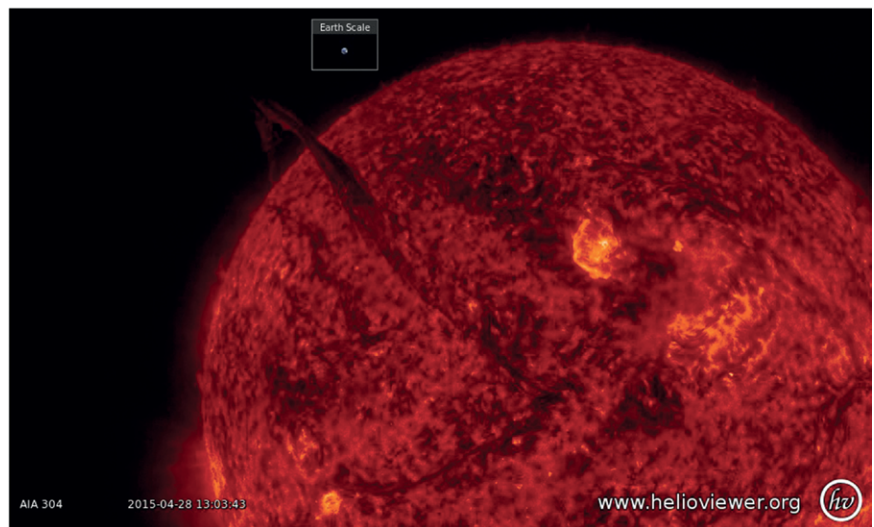


**FIG. 5.** A dark streak across the disk marks the presence of a huge filament stretching from the Sun's center to above the limb. The image is taken in He II (30.4 nm) by the NASA SDO AIA instrument on 28 Apr 2015. It was later observed to erupt, producing a spectacular coronal mass ejection moving away from the Sun at a velocity of nearly  $600 \text{ km s}^{-1}$  (see [www.youtube.com/watch?v=tXwQ46FEB\\_s](https://www.youtube.com/watch?v=tXwQ46FEB_s)).

energy is needed to heat the plasma to very high temperatures. How the Sun generates and dissipates this energy is still not well understood. The source of coronal heating remains one of the most elusive unsolved problems in astrophysics.

Another coronal mystery involves measured changes in elemental abundances. The solar composition is different in the corona than in the photosphere. Without knowing the elemental abundances with reasonable accuracy, it becomes impossible to derive many important physical parameters in coronal structures (e.g., the density, temperature, mass, and energetics). This difference is related to the first ionization potential (FIP) of the element (Laming 2015). Low-FIP (more easily ionized) elements like iron are enhanced with respect to their photospheric abundance values, and high-FIP elements like the noble

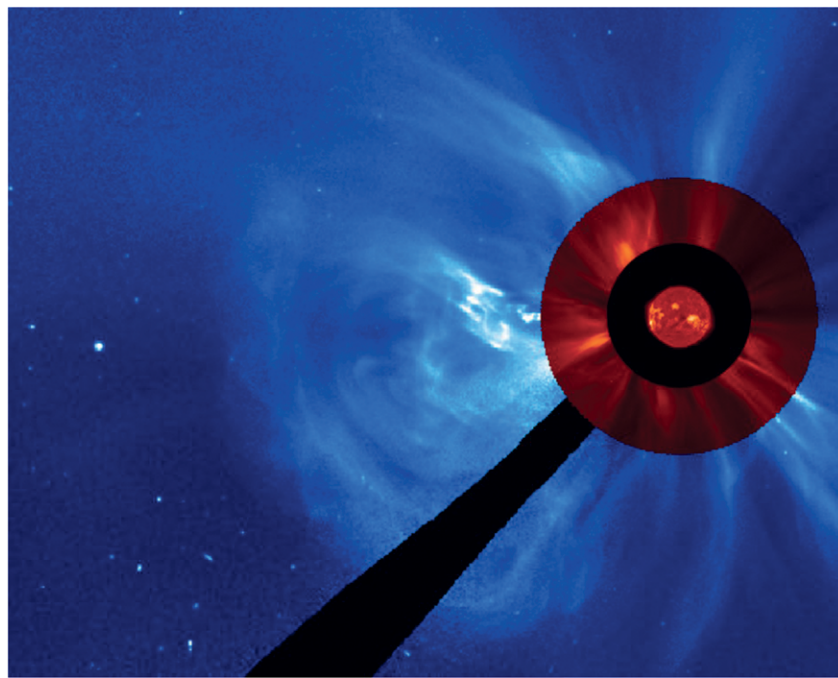


**FIG. 6.** The CME is the bright bubblelike feature visible at 9 o'clock above the occulting disk's support arm. It came from the X5 flare at 0208 UTC 25 Feb 2014 (see Fig. 1). This CME propagated away from the Sun with velocities of up to  $1,500 \text{ km s}^{-1}$ . This is a composite picture of He II (30.4 nm) from SDO AIA, showing the solar disk, and the Large Angle and Spectrometric Coronagraph (LASCO) C2 and C3 instruments on SoHO.

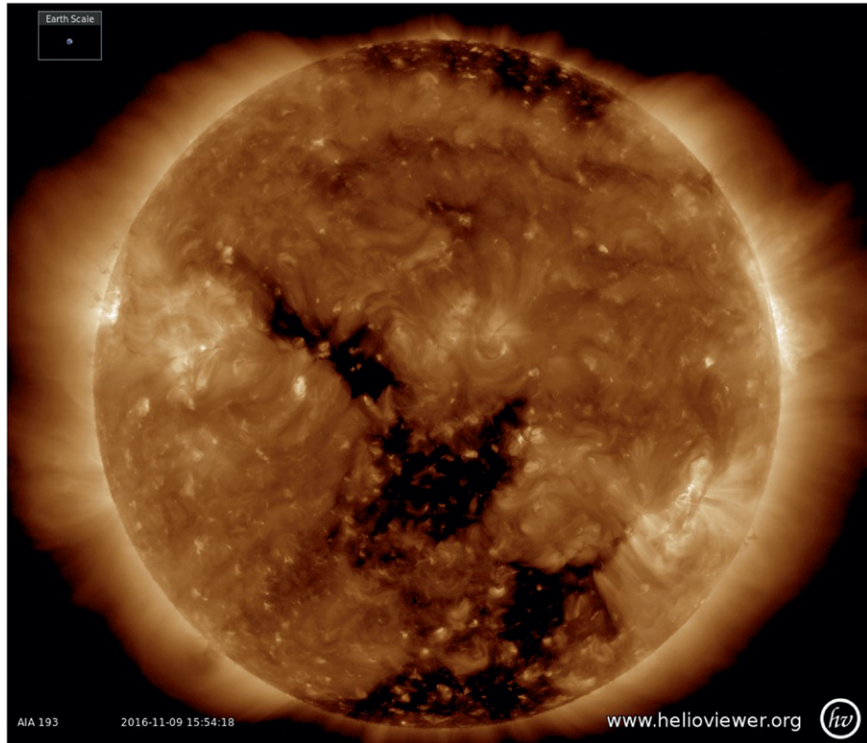


**FIG. 7.** A coronal hole stretching from the southern pole to across the solar equator, as seen in Fe XII (19.3 nm; 1.2 MK) at 1554 UTC 9 Nov 2016. Both the northern and southern polar coronal holes are visible. Note the intricate web of faint magnetic loops across much of the solar disk, with brighter loops associated with higher-temperature and -density coronal active regions located above the strong fields around sunspots. (Source: NASA SDO AIA.)

gases are depleted. This differentiation is most likely related to the magnetic field and begins at lower layers of the solar atmosphere where the low-FIP elements are charged and therefore are channeled by the magnetic field while high-FIP elements remain neutral and so their circulation remains unhindered by the fields. The details of the mechanics are as yet unknown, but this FIP effect extends out beyond the corona and in the solar wind out into interplanetary space (Schmelz et al. 2012). This same effect is observed in other solarlike stars (Wood and Laming 2013).

Flares and CMEs are often confused. They are both the result of the reconfiguration of the coronal magnetic fields that can become unstable and lead to a sudden and catastrophic release of stored magnetic energy. A flare can occur without a significant ejection of plasma. A CME can occur without a large flare. The most potent space weather effects are often observed when a large flare occurs with an accompanying CME. The primary difference between flares and CMEs is in the form that the energy release takes.

**FLARES.** Flares release energy in a number of different ways: electromagnetic radiation from 100-MeV  $\gamma$  rays to long-wavelength ( $>10$  m) radio emissions, particle acceleration, ejecta, and blast waves. The main energy release is in the form of heating of plasma to temperatures of 20 MK or higher (greater than the temperatures in the solar core!), with the resulting isotropic emission of the electromagnetic radiation.

The solar energy output is about  $4 \times 10^{26}$  J s $^{-1}$ . The total energy released in a typical flare is about  $10^{20}$  J. The largest observed flares may have emitted as much as  $10^{25}$  J, but such large flares are generally long-duration events so that their energy output is spread over many hours. Thus, the instantaneous increase in total solar output from such extreme events

would be negligible. It has been calculated that the maximum radiant energy released by solar flares cannot exceed about  $10^{27}$  J (Aulanier et al. 2013). However, other solarlike stars have been observed to produce flares several orders of magnitude larger than those detected on the Sun (Hiroyuki et al. 2012).

Active regions are areas of strong magnetic field where most flares occur. They appear as clusters of sunspots in the photosphere, regions of plage in the chromosphere, and concentrations of bright X-ray loops in the corona. Plages are bright chromospheric regions often observed near sunspots and are related to similar bright areas often seen in the photosphere, called faculae. They play an important role in the solar irradiance variability (Part I). The increased presence of plage during solar maximum increases the UV, EUV, and X-ray flux incident on Earth's atmosphere (Krivova et al. 2009).

Since the magnetic loops are anchored in the photosphere, the dynamics of differential rotation and convection (Part I) can drag and stretch the field lines until they are in configurations that are very far from equilibrium. At some catastrophic point,

the loop system collapses, releasing huge amounts of magnetic energy in a short time. The disrupted field lines reconnect as the region settles back into a configuration closer to equilibrium. (Magnetic reconnection occurs when stressed opposing fields recombine into a simpler, lower-energy configuration.) It is this released energy that produces both flares and CMEs.

Active regions are surrounded by areas of quiet sun, which are nonetheless quite dynamic. In the quiet sun, the magnetic fields are weaker, even small sunspots are rare, and the magnetic loops are significantly shorter. The quiet sun and coronal holes are punctuated by small X-ray bright points, which are always associated with simple magnetic dipoles in the photosphere and dark ephemeral regions in the chromosphere. These bright points are thought to be the smallest magnetically driven regions in the corona, being simply miniature versions of active regions. The active regions and their associated phenomena drive much of the short-term space weather effects.

The most commonly used and simplest flare classification is the X-ray flare classification from the National Oceanic and Atmospheric Administration's (NOAA) Space Weather Prediction Center, which assigns to each event a letter (A, B, C, M, X) and a number (1–10) in a logarithmic scale based on the flare's X-ray output in the 0.1–0.8-nm band. An A1 flare is defined as having a flux of  $10^{-5}$  W m $^{-2}$ . A B1 flare would be 10 times brighter and so on. There is no category above X, so a flare 20 times brighter than an X1 flare is classified as an X20 event.

Flares are also classified according to their duration. Short-burst flares are called impulsive flares and are generally typical of rapidly emerging or dynamic sunspots. Such flares can increase the X-ray intensity of the entire Sun by four orders of magnitude in a few minutes. Flares that last several hours are indicative of the formation of postflare loops that result from the reconfiguration of the coronal magnetic field following the launch of a CME away from the Sun; these are termed long-duration events (LDEs).

One hypothesis often suggested to be a solution to the coronal heating problem is the existence of myriads of tiny flares occurring continuously as the solar magnetic fields interact on very small spatial and temporal scales; these flares are called nanoflares (Klimchuk 2006).

Large flares can accelerate particles, primarily electrons and protons, to near relativistic velocities. This is relatively rare, but when it happens, Earth can be bathed in a stream of high-energy particles called

a radiation storm. Such events can also emit large quantities of gamma rays.

Long-term forecasting of solar activity is currently beyond our reach, rather like forecasting Earth's climate was 50 years ago. But can we predict flares even a few hours in advance? Not really, but some progress has been made in the statistical forecasting of flare events (Falconer et al. 2011). The advent of the Solar Dynamics Observatory (SDO) has provided continuous vector magnetic field imaging of the photosphere. Machine-learning algorithms used on these data have provided higher true skill statistical scores when predicting M- and X-class flares and CMEs (Bobra and Couvidat 2015; Bobra and Ilonidis 2016).

There are several factors that indicate a high likelihood of a flare occurring:

- the rapid emergence of strong magnetic fields, especially in the vicinity of existing magnetic structures;
- sunspot dynamics—linear motions that lead to the collision of opposite-polarity regions or rotating spots that twist and stress the fields;
- the availability of free magnetic energy—from twisted or stretched magnetic fields nearly parallel to the magnetic neutral line; and
- active regions with strong magnetic fields of opposite polarity mixed together.

However, even with all these factors present there are many false alarms and missed events.

The idea of using precursor warning to capture the early stages of large flares was briefly experimented with during the Solar Maximum Mission (SMM) but without much success. There are many brightenings prior to the onset of a flare, but these are generally indistinguishable from the ordinary dynamics of an active region. The best rule of thumb for flare forecasting is that if a major flare has just occurred, there is an increased probability of another one within a day or so.

Radiation from flares can directly heat the upper layers of Earth's atmosphere, causing the scale height and neutral density of the atmosphere to increase. This can shorten the life of low-Earth-orbiting satellites as a result of an increase in orbital drag. The increased UV emission can affect the chemistry and thus the dynamics of these layers too. It is not clear that flares have any direct or indirect effects on Earth's tropospheric weather or climate. Particles accelerated by flares can degrade imaging systems even in Earth orbit and could pose a danger to astronauts outside Earth's magnetic shield, the magnetosphere.

**CORONAL MASS EJECTIONS.** CMEs (see, e.g., Fig. 6) are observed using a white-light coronagraph, which is a telescope that effectively produces an artificial total solar eclipse, blocking the light from the photosphere of the Sun and recording the faint light that is visible because of the scattering of photons off of electrons in the corona. Regular space-based observations from the SMM, Solar and Heliospheric Observatory (SoHO), Solar Mass Ejection Imager, and Solar Terrestrial Relations Observatory (STEREO) have provided an extensive database of CME characteristics since 1980. The combination of observations from several different vantage points improves knowledge of the three-dimensional structure of CMEs. Such observations reveal significant variation in CME properties (Webb and Howard 2012).

The sizes and shapes of CMEs vary, with widths from  $10^\circ$  to  $300^\circ$ , excluding halo CMEs (Gopalswamy 2004). The average width is about  $50^\circ$ . A halo CME is one that is heading directly toward or away from Earth, thus producing a ring effect when observed with a coronagraph.

The velocities of most CMEs range from  $<100$  to  $2,200 \text{ km s}^{-1}$  with an average of about  $500 \text{ km s}^{-1}$  (Gopalswamy et al. 2010). CMEs are often observed to accelerate as they move away from the Sun. Slow CMEs tend to accelerate whereas fast ones decelerate. In either case, this is likely due to their interactions with the solar wind, which has a velocity from 300 to  $800 \text{ km s}^{-1}$  (St. Cyr et al. 2000).

According to Vourlidas et al. (2010), the mass of a CME ranges from  $10^8$  to  $10^{14} \text{ kg}$ . The uncertainties in CME masses are large, so the amount of energy in a CME is also poorly known but is between  $10^{21}$  and  $10^{23} \text{ J}$ , which, even with the uncertainties, dwarfs most flare energies. The amount of mass lost by the Sun in CMEs averaged over a solar cycle is less than 1% of that exported by the solar wind.

CME properties (size, mass, velocity, and magnetic field) vary with the solar cycle. The larger, faster, and more energetic CMEs typically occur near solar maximum, and the smaller, slower, and less energetic ones occur near solar minimum. The frequency of CMEs also varies throughout the cycle. At solar maximum CMEs are observed to occur at a rate of about five per day, whereas at solar minimum they are 20 times less frequent (Gopalswamy 2004).

The most obvious feature of a CME is a bright front moving out from the Sun that can expand to be many times the size of the Sun. Immediately behind the front is a darker region called a void, and imbedded within the void there is sometimes a bright

filamentary structure, a remnant of the erupting filament. The front is thought to be a shock driven by the CME. These shocks can also accelerate protons to near-relativistic velocities and cause extended proton events on Earth.

The appearance of a CME is greatly affected by where it occurs on the Sun with respect to the observer. The observed scattered light is optimal in the plane of the sky, so CMEs on the solar limb are most plainly observed, while a similar CME on the disk (seen at a less favorable angle) would appear fainter.

Unlike flares, which emit radiant energy isotropically, CMEs are directional. Thus, major eruptions on the Sun can miss Earth entirely. This makes predictions of their geoeffectiveness problematic. To predict the effects, the CME velocity, density, and magnetic configuration must be known. The size, location, and velocity of an event can generally be fairly well established, which one might think would enable a forecaster to determine whether Earth lies in its path and predict an accurate arrival time. However, the characteristics of the solar wind through which the CME will pass are generally unknown, so the unknown amount of acceleration or deceleration increases the uncertainty on its arrival time.

Different parts of a CME will have different densities, velocities, and magnetic field characteristics. Earth is a tiny target compared to the structure of the CME, so it is not known which feature of the CME will strike the planet. Further, for a CME to be optimally geoeffective, the vertical (north-south) component  $B_z$  of the CME's magnetic field must have the opposite polarity to that of Earth's field, so it can reconnect more efficiently. There is no detailed foreknowledge of these parameters or of the nature of any particles accelerated by them until the CME front passes sentinel spacecraft located at the L1 point, about  $1.5 \times 10^6 \text{ km}$  on the sunward side of Earth. The warning time depends critically on the velocity of the CME; it is the high-speed CMEs that are of most concern. Thus, a CME traveling at about  $400 \text{ km s}^{-1}$  will be detected about an hour before it impacts Earth, which is usually enough time to safe power and satellite systems. However, some CMEs can travel at over  $1,000 \text{ km s}^{-1}$ , giving little or no warning time. A CME was recorded by STEREO to be traveling at up to  $2,200 \text{ km s}^{-1}$ , which would give a bare 10-min warning!

Although the total energy of a CME often dwarfs that of any accompanying flare, the amount of energy transferred from the CME to Earth is negligible. This is because the CME energy is dissipated over

a huge volume of space and the energy density of CMEs is consequently low. Most of the energetic particles directed at Earth are diverted around the magnetosphere. The primary energy input to the magnetosphere comes from the dynamic pressure and electromagnetic energy transfer from the solar wind. The effect of that energy input is the energization of plasma and energetic particles, generation of currents, joule heating, and the precipitation of those particles into the ionosphere. Thus, any energy input to Earth is primarily directed in an oval region around the planet's magnetic poles. It has been estimated that this can amount to  $<0.01 \text{ W m}^{-2}$  (Wickwar Baron and Sears 1975; Knipp et al. 2004), which is insignificant compared to the total solar irradiance of about  $1,361 \text{ W m}^{-2}$ .

**CONCLUSIONS.** To be able to understand and eventually predict geoeffective space weather events on Earth, in interplanetary space, and on other planets, we must understand the physical mechanisms that drive both the long- and short-term variations of the Sun. The problem for those who study these solar phenomena is that our view of the Sun is incomplete and woefully undersampled in the spatial, spectral, and temporal domains, as will be discussed in Part III.

However, even if all the source drivers were comprehensively observed and perfectly understood, that would provide only a part of the space weather puzzle. These disturbances have to propagate through interplanetary space, where they interact with and are changed by the solar wind and planetary systems. The harsh environment of interstellar space also intrudes upon the solar system, penetrating the Sun's extended magnetic shield: the heliosphere. In Part III, we follow the journey of the solar wind from the upper layers of the solar atmosphere to the very edge of the solar system and show how it interacts with other bodies, including Earth, along the way.

**ACKNOWLEDGMENTS.** The authors thank the members of the Heliophysics Division at NASA GSFC for their help and support. The long-standing open-data policy of the Heliophysics community has enabled all solar researchers to investigate the effects of space weather in a more creative and cooperative way. Most solar images and movies can be easily created ([www.helioviewer.org/](http://www.helioviewer.org/)). Digital data can be downloaded from the Virtual Solar Observatory (<http://sdac.virtualsolar.org/>). The data can be analyzed using the SolarSoft software package. This work was supported in part by funding from the FedEx Institute of Technology at the University of Memphis.

## REFERENCES

- Asplund, M., N. Grevesse, A. J. Sauval, and P. Scott, 2009: The chemical composition of the Sun. *Annu. Rev. Astron. Astrophys.*, **47**, 481–522, doi:10.1146/annurev.astro.46.060407.145222.
- Aulanier, G., P. Démoulin, C. J. Schrijver, M. Janvier, E. Pariat, and B. Schmieder, 2013: The standard flare model in three dimensions: II. Upper limit on solar flare energy. *Astron. Astrophys.*, **549**, 66–75, doi:10.1051/0004-6361/201220406.
- Bobra, M. G., and S. Couvidat, 2015: Solar flare prediction using SDO/HMI vector magnetic field data with a machine-learning algorithm. *Astrophys. J.*, **798**, 135–146, doi:10.1088/0004-637X/798/2/135.
- , and S. Ilonidis, 2016: Predicting coronal mass ejections using machine learning methods. *Astrophys. J.*, **821**, 127–146, doi:10.3847/0004-637X/821/2/127.
- De Pontieu, B., and Coauthors, 2007: A tale of two spicules: The impact of spicules on the magnetic chromosphere. *Publ. Astron. Soc. Japan*, **59** (Suppl. 3), S655–S662, doi:10.1093/pasj/59.sp3.S655.
- Falconer, D., A. F. Barghouty, I. Khazanov, and R. Moore, 2011: A tool for empirical forecasting of major flares, coronal mass ejections, and solar particle events from a proxy of active-region free magnetic energy. *Space Wea.*, **9**, S04003, doi:10.1029/2009SW000537.
- Gopalswamy, N., 2004: A global picture of CMEs in the inner heliosphere. *The Sun and the Heliosphere as an Integrated System*, G. Poletto and S. T. Suess, Eds., Astrophysics and Space Science Library, Vol. 317, Kluwer, 201–251.
- , S. Akiyama, S. Yashiro, and P. Makela, 2010: Coronal mass ejections from sunspot and non-sunspot regions. *Magnetic Coupling between the Interior and the Atmosphere of the Sun*, S. S. Hasan and R. J. Rutten, Eds., Astrophysics and Space Science Proceedings, Springer, 289–307, doi:10.1007/978-3-642-02859-5\_24.
- Hiroyuki, M., and Coauthors, 2012: Superflares on solar-type stars. *Nature*, **485**, 478–481, doi:10.1038/nature11063.
- Klimchuk, J. A., 2006: On solving the coronal heating problem. *Sol. Phys.*, **234**, 41–77, doi:10.1007/s11207-006-0055-z.
- Knipp, D., W. Tobiska, and B. Emery, 2004: Direct and indirect thermospheric heating sources for solar cycles 21–23. *Sol. Phys.*, **224**, 495–505, doi:10.1007/s11207-005-6393-4.
- Krivova, N., S. Solanki, T. Wenzler, and B. Podlipnik, 2009: Reconstruction of solar UV irradiance since 1974. *J. Geophys. Res.*, **114**, D00I04, doi:10.1029/2009JD012375.

- Laming, J. M., 2015: The FIP and inverse FIP effects in solar and stellar coronae. *Living Rev. Sol. Phys.*, **12**, 1–74, doi:10.1007/lrsp-2015-2.
- Mackay, D. H., J. T. Karpen, J. L. Ballester, B. Schmieder, and G. Aulanier, 2010: Physics of solar prominences: II—Magnetic structure and dynamics. *Space Sci. Rev.*, **151**, 333–399, doi:10.1007/s11214-010-9628-0.
- Schmelz, J. T., 1999: The elemental composition of the solar corona: Abundance normalization and possible abundance variability. *Eighth SOHO Workshop: Plasma Dynamics and Diagnostics in the Solar Transition Region and Corona*, Paris, France, European Space Agency, 585–588.
- , D. Reames, R. Von Steiger, and S. Basu, 2012: Composition of the solar corona, solar wind, and solar energetic particles. *Astrophys. J.*, **755**, 33–39, doi:10.1088/0004-637X/755/1/33.
- St. Cyr, O. C., and Coauthors, 2000: Properties of coronal mass ejections: SOHO LASCO observations from January 1996 to June 1998. *J. Geophys. Res.*, **105**, 18 169–18 185, doi:10.1029/1999JA000381.
- Strong, K. T., J. L. R. Saba, and T. A. Kucera, 2012: Understanding space weather: The Sun as a variable star. *Bull. Amer. Meteor. Soc.*, **93**, 1327–1335, doi:10.1175/BAMS-D-11-00179.1.
- , N. Viall, J. T. Schmelz, and J. L. R. Saba, 2017: Understanding space weather. Part III: The Sun's domain. *Bull. Amer. Meteor. Soc.*, doi:10.1175/BAMS-D-16-0204.1, in press.
- Vourlidas, A., R. A. Howard, E. Esfandiari, S. Patsourakos, S. Yashiro, and G. Michalek, 2010: Comprehensive analysis of coronal mass ejection mass and energy properties over a full solar cycle. *Astrophys. J.*, **722**, 1522–1538, doi:10.1088/0004-637X/722/2/1522.
- Webb, D., and T. Howard, 2012: Coronal mass ejections: Observations. *Living Rev. Sol. Phys.*, **9**, 3, doi:10.12942/lrsp-2012-3.
- Wickwar, V., M. Baron, and R. Sears, 1975: Auroral energy input from energetic electrons and joule heating at Chatenika. *J. Geophys. Res.*, **80**, 4364–4367, doi:10.1029/JA080i031p04364.
- Wood, B., and J. M. Laming, 2013: The coronal abundances of mid-F dwarfs. *Astrophys. J.*, **768**, 122–132, doi:10.1088/0004-637X/768/2/122.

Dear AMS Community,

Since 1991, the American Meteorological Society Education Program (AMS Education) has been working on behalf of the AMS community to increase public scientific literacy. AMS Education offers a wide variety of resources, materials, and programs for K-12 educators as well as for faculty at undergraduate institutions. Our partnerships with NOAA, NASA, and NSF have allowed AMS Education to provide free professional development training workshops to K-12 teachers and undergraduate professors at minority serving institutions.

We welcome you to join us as we continue to support teachers nationwide. Please consider volunteering your expertise to a local implementation team teaching teachers or participating in a course held each fall and spring semester.

Sincerely,

Wendy Abshire  
Director  
AMS Education



Learn more: [ametsoc.org/DataStreme](https://ametsoc.org/DataStreme)

Questions: [amsedu@ametsoc.org](mailto:amsedu@ametsoc.org)